

# Peptide Plane Torsion Angles in Proteins through Intraresidue $^1\text{H}$ – $^{15}\text{N}$ – $^{13}\text{C}'$ Dipole–CSA Relaxation Interference: Facile Discrimination between Type-I and Type-II $\beta$ -Turns

Karin Kloiber and Robert Konrat\*

Institute of Organic Chemistry  
University of Innsbruck, Austria

Received June 27, 2000

Revised Manuscript Received October 9, 2000

Protein structures are built up from stretches of secondary structure elements,  $\alpha$  helices and  $\beta$ -sheets, linked together by loop regions varying in length and shape. Loop regions are typically located at the surface. Beyond their trivial function as connecting units between secondary structure elements, loop regions often form protein binding sites or enzyme active sites.<sup>1</sup> Despite their considerable functional importance, structural characterization of loop regions by solution NMR is still cumbersome. There is an increasing appreciation of cross-correlated nuclear spin relaxation in protein NMR spectroscopy.<sup>2–12</sup> In this work, we propose a method which measures intraresidue  $^1\text{H}(i)$ – $^{15}\text{N}(i)$ – $^{13}\text{C}'(i)$  dipole–chemical shift anisotropy (CSA) relaxation interference in  $^{13}\text{C}$ ,  $^{15}\text{N}$ -labeled proteins. This cross-correlation rate is sensitive to the orientation of the  $\text{N}(i)$ – $\text{H}(i)$  dipolar vector in the principal frame of the intraresidue  $^{13}\text{C}'(i)$  CSA tensor and can be efficiently used as an alternative to NOEs for the discrimination between type-I and type-II  $\beta$ -turns in proteins.

The pulse sequence is outlined in Figure S1 of the Supporting Information. The experiment is analogous to the HN(CA)CO scheme<sup>13</sup> in terms of the flow of magnetization. The main difference is a constant-time evolution delay  $T_C$ , during which differential relaxation of multiplet components of  $^{13}\text{C}'$ – $^{15}\text{N}$  multiple-quantum coherences is monitored, and the chemical shift of the carbonyl carbon is recorded. To improve the spectral resolution, simultaneous  $180^\circ$  pulses to the  $^{15}\text{N}$  and  $^1\text{H}$  nuclei in the middle of the constant time delay  $T_C$  were applied as proposed by Kay and co-workers,<sup>4</sup> leading to an HNCO-type cross-peak, centered at the intraresidue carbonyl frequency and split by the one-bond  $^{15}\text{N}$ – $^1\text{H}$  scalar coupling. To further increase the resolution 2-fold, we followed an approach that has been introduced by Yang and Nagayama<sup>14</sup> and more recently by Sørensen et al.<sup>15</sup> Two 3D data sets are recorded in which the

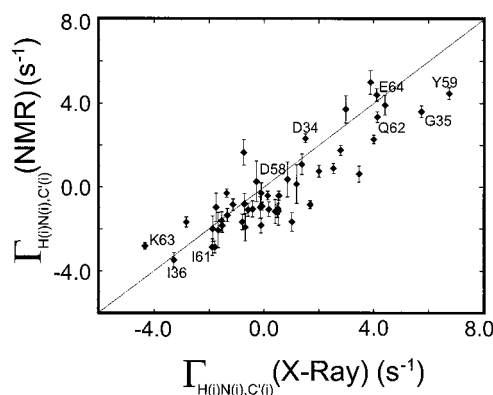


**Figure 1.** Correlation of calculated and experimental  $\Gamma_{\text{H}(i)\text{N}(i),\text{C}'(i)}$  values. A 1.5 mM ubiquitin sample,<sup>16</sup> 10 mM phosphate, pH = 5.6, 26 °C was employed, and a total measuring time of 24 h was used to record the 3D data set using the pulse sequence of Figure S1 [ $T_C = 30$  ms,  $25 \times 25 \times 512$  complex points with acquisition times of 21, 15, and 64 ms in ( $t_1$ ,  $t_2$ ,  $t_3$ )]. Triplicate data sets were measured and are given as average values. In the calculation values of 244, 178, and 90 ppm were employed for  $\sigma_{xx}$ ,  $\sigma_{yy}$ , and  $\sigma_{zz}$ , with  $x$  and  $y$  axes located in the peptide plane and the  $y$  axis of the CSA tensor rotated by  $8^\circ$  with respect to the carbonyl bond,<sup>17</sup> and using vector projections calculated from the crystal structure coordinates.<sup>18</sup> An overall correlation time  $\tau_C$  of 4.2 ns was assumed, additional internal dynamic was neglected.

one-bond  $^{15}\text{N}$ – $^1\text{H}$  scalar coupling modulation during  $t_1$  is modified (cosine or sine). Addition or subtraction of the two data sets results in two separate spectra where the cross-peaks are shifted by  $\pm^{1/2} J_{\text{NH}}$  in  $t_1$ . It is important to note that  $^{15}\text{N}/^{15}\text{N}$ – $^1\text{H}$  CSA-dipole cross-correlated relaxation during the second  $\tau_b$  period in the sine-modulated experiment (Figure S1B) leads to the build-up of  $^{15}\text{N}$  coherences which are in-phase with respect to  $^1\text{H}$ . This results in an underestimation of the experimental cross-correlation rate  $\Gamma_{\text{H}(i)\text{N}(i),\text{C}'(i)}$ . For ubiquitin ( $\Delta\sigma(^{15}\text{N}) = -160$  ppm;  $\tau_C = 4.2$  ns), we estimate a contribution of about  $-0.5 \text{ s}^{-1}$  to the experimental values. The cross-correlation rate  $\Gamma_{\text{H}(i)\text{N}(i),\text{C}'(i)}$  has a maximum value of about  $0.2 \text{ s}^{-1}$ , depending on the local backbone geometry. The values of  $\Gamma_{\text{H}(i)\text{N}(i),\text{C}'(i)}$  can be obtained in a straightforward manner from the intensity ratios of the downfield ( $I_{\text{df}}$ ) and upfield ( $I_{\text{uf}}$ ) multiplet components in the two resulting data sets, respectively. The cross correlation rate is given by

$$\Gamma_{\text{H}(i)\text{N}(i),\text{C}'(i)} = (0.5/T_C) \ln(I_{\text{uf}}/I_{\text{df}}) = \left( \frac{4}{15} \right) (h/2\pi) \gamma_{\text{H}} \gamma_{\text{N}} \omega_{\text{C}} (r_{\text{NH}})^{-3} \tau_{\text{C}} f(\sigma_x, \sigma_y, \sigma_z) \quad (1)$$

where  $\gamma_i$  is the gyromagnetic ratio of spin  $i$ ,  $r_{\text{NH}}$  is the distance between  $^1\text{H}$  and  $^{15}\text{N}$ ,  $\omega_{\text{C}}$  is the carbon Larmor frequency,  $\tau_{\text{C}}$  is the correlation time and  $\sigma_i$  is the  $i$ th principal component of the chemical shift tensor.  $f(\sigma_x, \sigma_y, \sigma_z)$  describes the relative orientation of the NH vector in the principal frame of the CSA tensor and can be calculated as a function of  $\varphi$  and  $\psi$ . Experimental data were recorded using  $^{13}\text{C}$ ,  $^{15}\text{N}$ -labeled ubiquitin. Figure 1 shows the correlation between experimental and theoretical cross-correlation rates. Theoretical rates were calculated on the basis of the available X-ray structure of ubiquitin<sup>18</sup> and using CSA parameters reported by Teng et al.<sup>17</sup> Part of the deviation is likely

\* To whom correspondence should be addressed. Institute of Organic Chemistry, University of Innsbruck, Innrain 52a, A-6020 Innsbruck, Austria. Fax: +43-512-507-2892. E-mail: robert.konrat@uibk.ac.at.

(1) Branden, C.; Tooze, J. *Introduction to Protein Structure*, 2nd ed.; Garland Publishing: New York, 1999.

(2) Reif, B.; Hennig, M.; Griesinger, C. *Science* **1997**, *276*, 1230–1233.

(3) Yang, D.; Konrat, R.; Kay, L. E. *J. Am. Chem. Soc.* **1997**, *119*, 11938–11940.

(4) Yang, D.; Gardner, K. H.; Kay, L. E. *J. Biomol. NMR* **1998**, *11*, 1–8.

(5) Yang, D.; Kay, L. E. *J. Am. Chem. Soc.* **1998**, *120*, 9880–9887.

(6) Pelupessy, P.; Chiarparin, E.; Ghose, R.; Bodenhausen, G. *J. Biomol. NMR* **1999**, *14*, 277–280.

(7) Chiarparin, E.; Pelupessy, P.; Ghose, R.; Bodenhausen, G. *J. Am. Chem. Soc.* **1999**, *121*, 6876–6883.

(8) Kloiber, K.; Konrat, R. *J. Biomol. NMR* **2000**, *17*, 265–268.

(9) Brutscher, B.; Skrynnikov, N. R.; Bremi, T.; Brüschweiler, R.; Ernst, R. R. *J. Magn. Reson.* **1998**, *130*, 346–351.

(10) Skrynnikov, N. R.; Konrat, R.; Muhandiram, D. R.; Kay, L. E. *J. Am. Chem. Soc.* **2000**, *122*, 7059–7071.

(11) Pellecchia, M.; Pang, Y.; Wang, L.; Kurichkin, A. V.; Kumar, A.; Zuiderweg, E. R. P. *J. Am. Chem. Soc.* **1999**, *121*, 9165–9170.

(12) Ghose, R.; Huang, K.; Prestegard, J. H. *J. Magn. Reson.* **1998**, *135*, 487–499.

(13) Clubb, R. T.; Thanabal, V.; Wagner, G. *J. Magn. Reson.* **1992**, *97*, 213–217.

(14) Yang, D.; Nagayama, K. *J. Magn. Reson., Ser. A* **1996**, *118*, 117–121.

(15) Sørensen, M. D.; Meissner, A.; Sørensen, O. W. *J. Biomol. NMR* **1997**, *10*, 181–186.

(16) Schneider, D. M.; Dellwo, M. J.; Wand, A. J. *Biochemistry* **1992**, *31*, 3645–3652.

(17) Teng, Q.; Iqbal, M.; Cross, T. A. *J. Am. Chem. Soc.* **1992**, *114*, 5312–5321.

(18) Vijay-Kumar, S.; Bugg, C. E.; Cook, W. J. *J. Mol. Biol.* **1987**, *194*, 531–544.

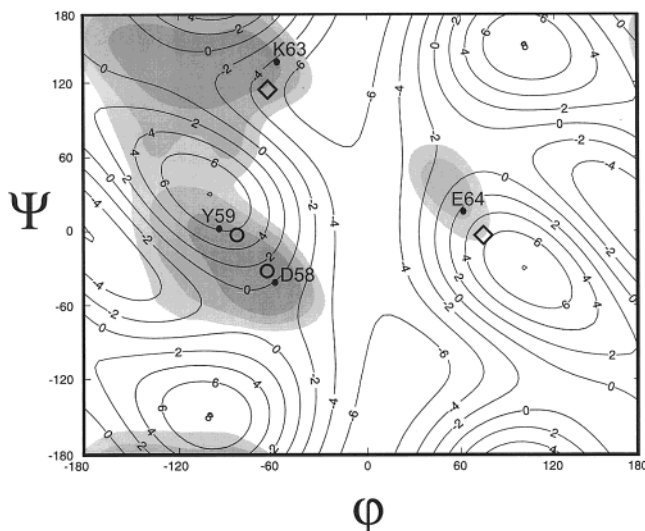


**Figure 2.**  $^1\text{H}-^{15}\text{N}-^{13}\text{C}'$  dipole-CSA cross-correlated relaxation  $\Gamma_{\text{H}(i)\text{N}(i),\text{C}'(i)}$  as a function of the intervening dihedral angles  $\varphi, \psi$ . CSA tensor and motional parameters (correlation time  $\tau_C$ ) were identical to those of Figure 1. Uniform backbone bond angles and bond distances were used.  $(\varphi, \psi)$  values for D58 ( $-55^\circ/-39^\circ$ ), Y59 ( $-91^\circ/5^\circ$ ), K63 ( $-54^\circ/143^\circ$ ) and E64 ( $67^\circ/19^\circ$ ) are denoted by filled circles. Allowed regions of  $\varphi, \psi$ -space are indicated by shading.<sup>20</sup>  $(\varphi, \psi)$  dihedral angles typical for the central pairs ( $i+1, i+2$ ) of successive residues in type-I ( $\varphi_{i+1} = -60^\circ, \psi_{i+1} = -30^\circ; \varphi_{i+2} = -90^\circ, \psi_{i+2} = 0^\circ$ ; open circles) and type-II ( $\varphi_{i+1} = -60^\circ, \psi_{i+1} = +120^\circ; \varphi_{i+2} = +90^\circ, \psi_{i+2} = 0^\circ$ ; diamonds)  $\beta$ -turns are also depicted.<sup>21</sup>

to be due to the assumption of a uniform  $^{13}\text{C}'$  CSA tensor and the neglect of internal dynamics. In general, rather small values are found for  $\alpha$ -helices ( $-0.06 \pm 1.7 \text{ s}^{-1}$ ) and  $\beta$ -sheets ( $-1.1 \pm 1.5 \text{ s}^{-1}$ ). In contrast, reasonably large values of  $|\Gamma_{\text{H}(i)\text{N}(i),\text{C}'(i)}|$  are measured for residues outside  $\alpha$ -helical or  $\beta$ -sheet regions of Ramachandran space (e.g., D34–I36; I61–E64; Figure S3). Additionally, consecutive residues in these regions typically show alternating signs for  $\Gamma_{\text{H}(i)\text{N}(i),\text{C}'(i)}$ . Residues D34–I36 are part of a loop connecting the  $\alpha$ -helix with a short  $3_{10}$  helix adjacent to  $\beta$ -strand III. The loop comprising residues I61–E64 links the second  $3_{10}$  helix with the terminal  $\beta$ -strand V. The X-ray<sup>18</sup> and NMR structure<sup>19</sup> of ubiquitin reported distinct local backbone geometries for the residue pairs D58/Y59 and K63/E64, respectively. The theoretical cross-correlation rates agree with experimental rates (see also Supporting Information), indicating that these distinct local backbone conformations are reasonably

(19) Cornilescu, G.; Marquardt, J. L.; Ottiger, M.; Bax, A. *J. Am. Chem. Soc.* **1998**, *120*, 6836–6837.

preserved in aqueous solution. The backbone dihedral angles  $\varphi, \psi$  for D58/Y59 are typical for the central residues ( $i+1, i+2$ ) of a type I  $\beta$ -turn, whereas  $\varphi, \psi$  values for K63/E64 are close to the values found for residues ( $i+1, i+2$ ) in a type II  $\beta$ -turn. Figure 2 indicates that  $\Gamma_{\text{H}(i)\text{N}(i),\text{C}'(i)}$  values obtained for the central pairs of consecutive residues ( $i+1, i+2$ ) in  $\beta$ -turns can thus be used to distinguish between the two  $\beta$ -turn conformations in proteins. For a type-I  $\beta$ -turn  $\Gamma_{\text{H}(i+1)\text{N}(i+1),\text{C}'(i+1)}/\tau_C$  (ns)  $\cong 0.0 \text{ s}^{-1}$  and  $\Gamma_{\text{H}(i+2)\text{N}(i+2),\text{C}'(i+2)}/\tau_C$  (ns)  $\cong +1.0 \text{ s}^{-1}$  are observed. In contrast, in the case of a type-II  $\beta$ -turn values on the order of  $-1.0$  and  $+1.0 \text{ s}^{-1}$  are obtained for  $\Gamma_{\text{H}(i+1)\text{N}(i+1),\text{C}'(i+1)}/\tau_C$  (ns) and  $\Gamma_{\text{H}(i+2)\text{N}(i+2),\text{C}'(i+2)}/\tau_C$  (ns), respectively.

In summary, a pulse sequence has been presented for measuring intraresidue  $^1\text{H}(i)-^{15}\text{N}(i)-^{13}\text{C}'(i)$  dipole–chemical shift anisotropy (CSA) relaxation interference in  $^{13}\text{C}, ^{15}\text{N}$ -labeled proteins. The experiment can be used to extract peptide plane torsion angles in loop or turn regions. Sensitivity consideration suggests, that due to the beneficial  $^{13}\text{C}^\alpha$ -relaxation in  $^2\text{H}$ -labeled proteins, the experiment is particularly suited to discriminate between type-I and type-II  $\beta$ -turns in large proteins, which require extensive deuteration and where only a limited number of NOEs are available. The method can also be applied to enzyme ligand systems<sup>22,23</sup> in the context of SAR by NMR<sup>24</sup> and may provide valuable structural information about local turn conformations in protein recognition sites.<sup>25</sup>

**Acknowledgment.** This paper is dedicated to Professor Horst Kessler on the occasion of his 60th birthday. The authors thank Professor A. Joshua Wand (University of Pennsylvania) for kindly supplying uniformly  $^{13}\text{C}, ^{15}\text{N}$ -labeled ubiquitin. R.K. thanks Professor Bernhard Kräutler (University of Innsbruck) for his continuous support and encouragement. This research was supported by Grant P 13486 from the Austrian Science Foundation FWF.

**Supporting Information Available:** Pulse sequence, representative spectra, and experimental details for the measurement of  $\Gamma_{\text{H}(i)\text{N}(i),\text{C}'(i)}$ , a table of experimental and calculated  $\Gamma_{\text{H}(i)\text{N}(i),\text{C}'(i)}$  rates based on the X-RAY and NMR structures, respectively (PDF). This material is available free of charge via the Internet at <http://pubs.acs.org>.

JA002314S

(20) Koradi, R.; Billeter, M.; Wüthrich, K. *J. Mol. Graphics* **1996**, *14*, 51–55.

(21) Sibanda, B. L.; Thornton, J. M. *Nature* **1985**, *316*, 170–174.

(22) Blommers, M. L. J.; Stark, W.; Jones, C. E.; Head, D.; Owen, C. E.; Jahnke, W. *J. Am. Chem. Soc.* **1999**, *121*, 1949–1953.

(23) Carlomagno, T.; Felli, I. C.; Czech, M.; Fischer, R.; Sprinzl, M.; Griesinger, C. *J. Am. Chem. Soc.* **1999**, *121*, 1945–1948.

(24) Shuker, S. B.; Hajduk, P. J.; Meadows, R. P.; Fesik, S. W. *Science* **1996**, *274*, 1531–1534.

(25) Rose, G. D.; Gierasch, L. M.; Smith, J. A. *Adv. Protein Chem.* **1985**, *37*, 1–109.